Title

Three Mutations Convert the Selectivity of a Protein Sensor from Nicotinic Agonists to S-Methadone for Use in Cells, Organelles, and Biofluids

Journal

Journal of the American Chemical Society, 144(19)

ISSN

0002-7863

Authors

Muthusamy, Anand K
Kim, Charlene H
Virgil, Scott C
et al.

Publication Date

2022-05-18

DOI

10.1021/jacs.2c02323

Peer reviewed

JACS
JOURNAL OF THE AMERICAN CHEMICAL SOCIETY
pubs.acs.org/JACS
Communication

Three Mutations Convert the Selectivity of a Protein Sensor from Nicotinic Agonists to S-Methadone for Use in Cells, Organelles, and Biofluids

Anand K. Muthusamy, Charlene H. Kim, Scott C. Virgil, Hailey J. Knox, Jonathan S. Marvin, Aaron L. Nichols, Bruce N. Cohen, Dennis A. Dougherty, Loren L. Looger, and Henry A. Lester*

Cite This: J. Am. Chem. Soc. 2022, 144, 8480−8486
Read Online

ABSTRACT: We report a reagentless, intensity-based S-methadone fluorescent sensor, iS-methadoneSnFR, consisting of a circularly permuted GFP inserted within the sequence of a mutated bacterial periplasmic binding protein (PBP). We evolved a previously reported nicotine-binding PBP to become a selective S-methadone-binding sensor, via three mutations in the PBP's second shell and hinge regions. iS-methadoneSnFR displays the necessary sensitivity, kinetics, and selectivity—notably enantioselectivity against R-methadone—for biological applications. Robust iS-methadoneSnFR responses in human sweat and saliva and mouse serum enable diagnostic uses. Expression and imaging in mammalian cells demonstrate that S-methadone enters at least two organelles and undergoes acid trapping in the Golgi apparatus, where opioid receptors can signal. This work shows a straightforward strategy in adapting existing PBPs to serve real-time applications ranging from subcellular to personal pharmacokinetics.

We report the first selective real-time fluorescent biosensor for a small molecule opioid, "intensity-based S-methadone sensing fluorescent reporter" or "iS-methadoneSnFR" (Figure 1). To employ the indicator for quantitative dynamic opioid measurements in cells and biofluids, we engineered iS-methadoneSnFR to meet necessary criteria: (1) sensitivity in the pharmacological range, (2) selectivity against endogenous molecules, (3) selectivity against exogenous drugs, including those of the same drug class, (4) photostability for the duration of measurements, (5) physical stability outside cells, and (6) reversible binding with ∼ second resolution.

The risk of opioid-use disorder and death by overdose has increased alongside the worldwide access to highly potent opioid agonists.[1] Nevertheless, opioids remain essential analgesics. Since the 1960s, methadone maintenance therapy (MMT) has served to reduce harm from opioid addiction.[2,3] MMT relies on pharmacokinetics: oral methadone's onset is slower than that of injected or inhaled μ-opioids, and its effects last much longer due to a ∼24 h half-life.[4] Therefore, despite acting as a μ-opioid agonist, methadone staves off withdrawal symptoms without producing the euphoria associated with other agonists.[4] However, interindividual variability in the metabolism of methadone, partially due to polymorphisms in cytochrome P450 isotypes,[5,6] can lead to therapeutic failures.[7] Methadone is clinically administered as the racemate and measuring either enantiomer is suitable for therapeutic drug monitoring.[8] Drug metabolism is conventionally addressed by blood draw, but this method is laborious, invasive, and restricted to the clinic. An optimal methadone readout would enable personalized dosing regimens, by producing real-time tracking of [methadone] in biological fluids and facilitating tapering from potent opioids. Within a subject, opioid pharmacokinetics also vary at the level of intracellular compartments to produce acid trapping and diverse interactions with receptors including chaperoning and activation.[9−11] In both cases, a sensor with in situ readout and ∼ second resolution is required.

Conventional small molecule detection methods have been extended to methadone but may be limited in specificity, temporal resolution, or spatial resolution.[12] An antibody against methadone was used in a lateral flow test of human sweat (limited to a single time point).[13] Electrochemical methods provide continuous measurements but vary in selectivity against other opioids[14−16] and, in all cases, cannot be used for subcellular measurements. A pioneering de novo protein design campaign for an opioid sensor, the binding of fentanyl produced a conformational switch in a transcription factor[17] but required a cellular readout and hours-to-days temporal resolution.

We hypothesized that all the required criteria could be satisfied by a single-chain sensor comprising a mutated bacterial periplasmic binding protein (PBP), a variant of the choline-binding protein OpuBC from *Thermoanaerobacter sp513*, interrupted by a circularly permuted GFP (cpGFP) (Figure 1).[18−20] The cpGFP insertion approach has also been

Received: March 1, 2022
Published: April 21, 2022

https://doi.org/10.1021/jacs.2c02323
J. Am. Chem. Soc. 2022, 144, 8480−8486

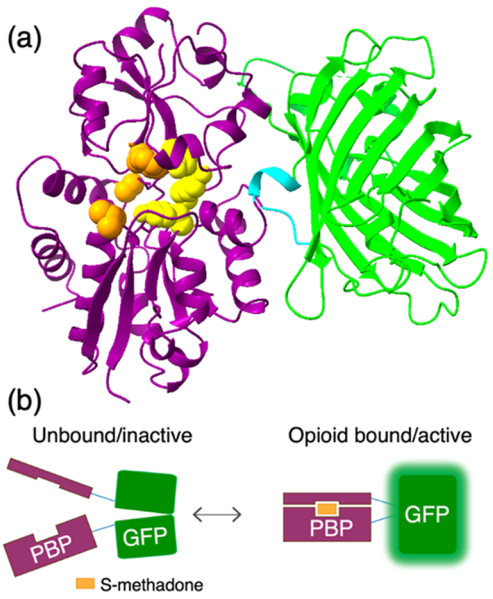

Figure 1. (a) Crystal structure of iNicSnFR3a (PDB:7S7T) mutated in silico to iS-methadoneSnFR (mutations shown in orange spheres). All but one putative cation−π residue in iNicSnFR3a were maintained in iS-methadoneSnFR's binding pocket (critical residues Y65, Y357, and Y460 shown as yellow spheres). (b) Biosensor mechanism: in the unbound state, GFP's chromophore has a poor environment for fluorescence. The PBP binds S-methadone with a "Venus fly trap" conformational change, increasing the brightness of the GFP chromophore.

used in Ca^{2+} sensors (the GCaMP series) and in neurotransmitter sensors.[18,21] Our strategy consisted of (1) screening each methadone enantiomer against a previously reported nicotine biosensor, iNicSnFR3a, and its variants[19] and (2) iterative site-saturation mutagenesis to select for S-methadone and against cholinergic ligands (Figure 2a). We performed chiral resolution on racemic methadone to isolate (+)-S-methadone and (−)-R-methadone (assigned by optical rotation[22]) with analytical purity and 99% enantiomeric excess (Figure S1).

While there is no structural homology or pharmacological overlap between nicotinic and μ-opioid receptors, several variants of nicotinic drug biosensors displayed weak fluorescence responses to S-methadone (Figure 2b). Although the PBP had no enantioselective pressure for binding its achiral ligand choline, all variants screened to date displayed enantioselectivity for S-methadone (Figure S2). Dose−response relations were fit to the Hill equation to determine an EC_{50} and $\Delta F_{max}/F_0$. In the linear portion of the dose−response relation we define the increase in fluorescence per micromolar, "S-slope", as a metric of biosensor sensitivity: $(\Delta(F/F_0)/(\Delta[\text{ligand}])$ at $[\text{drug}] \ll EC50$[23]). For a Hill coefficient of ∼1.0, the S-slope equals the ratio $(\Delta F_{max}/F_0)/EC_{50}$. A variant of iNicSnFR3a, iNicSnFR3b, provided the largest dynamic range for both S-methadone and R-methadone (Figure S2) and served as the input to several rounds of directed evolution.

We selected for both an increase in sensitivity to S-methadone and a decrease in sensitivity to nicotinic ligands. We chose mutation sites based on a crystal structure of iNicSnFR1 (PDB:6EFR) and directed evolution of iNicSnFR3a.[14] The resulting sensor displayed a ∼16-fold improvement in sensitivity over iNicSnFR3a; $\Delta F/F_0$ increased to 3.76 ± 0.16 at 1 μM, the representative plasma maintenance concentration[8] (Figure 2b). Notably, iS-methadoneSnFR displayed sensitivity to S-methadone that exceeded the sensitivity for any of the original cholinergic ligands and displayed a marked shift in ligand selectivity (Figure 2c). iS-methadoneSnFR displayed near-zero response for physiologically or pharmacologically relevant steady-state acetylcholine (ACh), choline, varenicline, and nicotine concentrations (∼1 μM, 10 to 20 μM,[24] 0 to 100 nM,[25] and ∼25 to ∼500 nM, respectively[26] (see Figure 4a)).

We characterized iS-methadoneSnFR's binding using docking and biochemical studies. Although only three mutations were required to generate iS-methadoneSnFR from iNicSnFR3a/3b, advantageous mutations were rare: ∼1% of all mutations screened were accepted as improvements. Docking S-methadone into recently reported structures of liganded iNicSnFR3a[27] showed that the *N*-methyl groups of S-methadone lie 4.6 and 5.5 Å from the aromatic groups of Y357 and Y65, respectively (slightly greater than the distance from the beta carbons of varenicline to these two groups). In the initial round of mutations, most sites yielded no improvement, except for a W436F mutation spatially near Y65 and Y357 (Figure S3). We previously reported nicotine and varenicline making cation−π interactions with Y65 and Y357 in iNicSnFR3a (PDB:7S7T and 7S7U, respectively).[27] Each nicotinic ligand bears a protonated nitrogen lying midway on the axis of the aromatic centroids of Y65 and Y357 (Figure 3a). In the subsequent round, second-shell mutation N11V created additional volume next to F12, in the second shell. Finally, the third round yielded L490A, allowing for greater flexibility in the hinging of the PBP.

Leucine mutagenesis among individual binding pocket aromatic residues showed the primacy of Y65, Y357, F12, and Y460 (Figure 3b). An aromatic side-chain screen across these four positions revealed a necessity of Tyr in the first shell positions Y65, Y357, and Y460 (Figure 3c). Substituting a noncanonical side chain, O-methyltyrosine, yielded a near-null biosensor at residue 65 but not at 12 (Figure S4). These data suggest that S-methadone's amine directly interacts with the first shell residues, as with nicotinic drugs, and the phenolic −OH is necessary for hydrogen bonding. The three accepted mutations represent a 94 $Å^3$ reduction in van der Waals' volume, comparable to the 132 $Å^3$ increase in ligand volume from varenicline to methadone, as though the accepted mutations allowed S-methadone better access to aromatic residues critical to binding both classes of drugs. Therefore, the PBP has an aromatic binding pocket for protonated amines, and other regions of the binding site can be tuned to accommodate the remainder of the ligand's steric bulk and functional groups.

iS-methadoneSnFR satisfied our sensitivity, selectivity, and biophysical criteria for a useful biosensor. Fluorescence dose−response relations showed an excellent dynamic range, $\Delta F_{max}/F_0$ of 15.3 ± 0.2, and an EC_{50}, 3.2 ± 0.2 μM, near the relevant plasma concentrations for maintenance therapy.[8] Isothermal titration calorimetry (ITC) determined a K_d of 1.9 ± 0.2 μM, in good agreement with the fluorescence EC_{50} (Figure 4c). ITC also demonstrated a single binding site (stoichiometry = 0.92) with an entropically driven conformational change. iS-methadoneSnFR had little or no response (S-slope < 0.1 μM^{-1}) to other neurotransmitters (Figure 4a) and other opioids (Figure 4b). The S-slope for S-methadone was ∼20× that for R-methadone. When we added R-methadone to S-

https://doi.org/10.1021/jacs.2c02323
J. Am. Chem. Soc. 2022, 144, 8480−8486

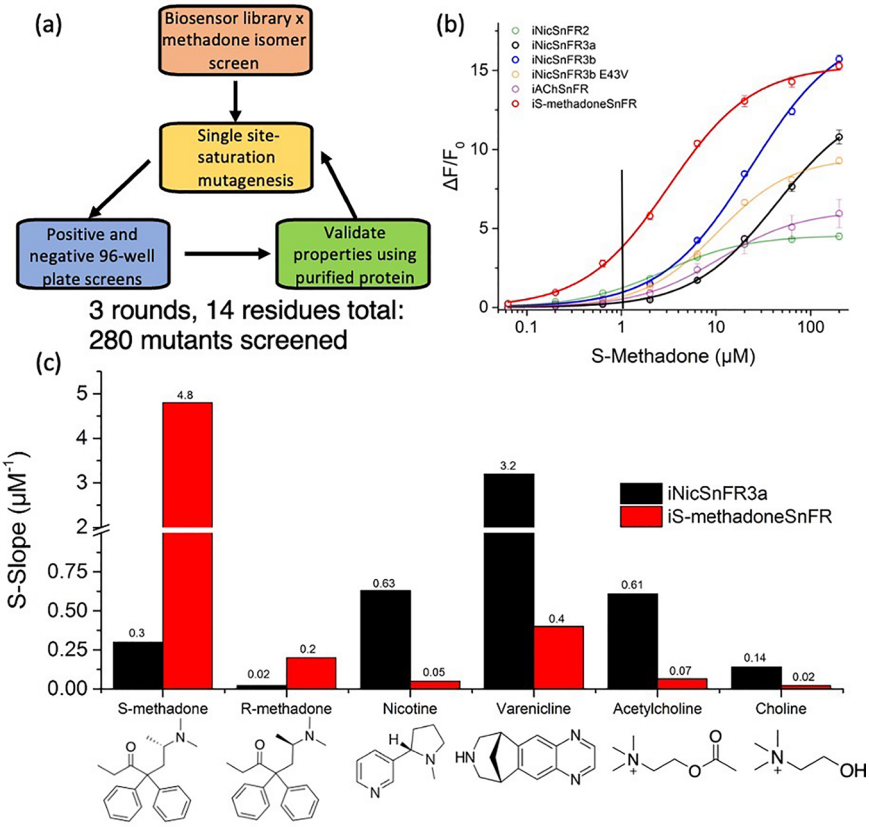

Figure 2. (a) Directed evolution strategy. (b) Fluorescence responses to S-methadone. iNicSnFR3a (black) has several variants (faded curves), of which one has markedly better sensitivity, owing to the N11E mutation (blue). This lead was evolved to iS-methadoneSnFR (red), which included reoptimization at position 11. Only the final biosensor had sufficient sensitivity at 1 μM (vertical black line; the relevant maintenance concentration). (c) Shift in selectivity from iNicSnFR3a (black) to iS-methadoneSnFR (red) measured by S-slope (see text). Note the scale change at the axis break.

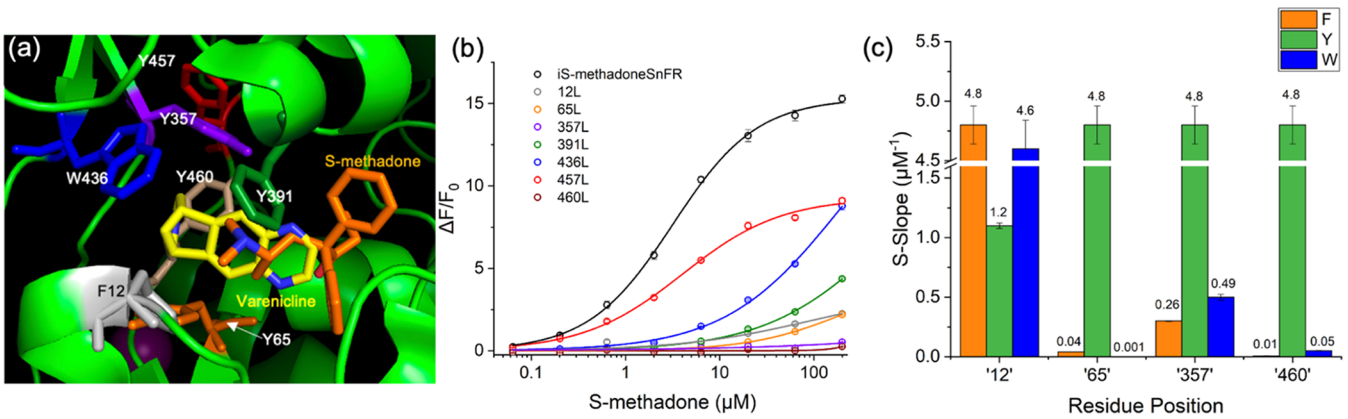

Figure 3. (a) PDB:7S7T(iNicSnFR3a, varenicline bound) showing cation−π interactions with Y65 and Y357. S-methadone was docked into 7S7T. (b) Fluorescence dose−response relations of cation−π residue Leu mutants. (c) Aromatic side-chain screen through critical positions identified in (b) with resulting S-slope. Note the break in y-axis.

methadone, fluorescence was modestly elevated at lower [S-methadone], but all responses converged at the $\Delta F_{max}/F_0$ for S-methadone alone (Figure S5). 1-s stopped flow kinetics were obtained using racemic methadone (Figure S4) and determined an apparent k_{on} of 0.13 μM^{-1} s^{-1} (Figure 4d). The final 10 ms of the 1 s stopped-flow traces were fitted by a Hill equation with $EC_{50} \sim 8$ μM (Figure S6) for the racemate, which was approximately double the EC_{50} for S-methadone alone (as expected if the binding strongly favors the S-enantiomer).

Therapeutic use of opioids would be improved by quantitative, real-time, minimally invasive or noninvasive measurements in sweat, saliva, and interstitial fluid.[28,29] The selectivity and high aqueous solubility of iS-methadoneSnFR enable its use in such applications. We tested the biosensor in PBS:biofluid samples and found robust responses in the pharmacologically relevant concentration range (Figure 5). iS-methadoneSnFR, like all GFP-based biosensors, displays smaller responses at pH < ~7 (Figure S7). Because biofluids, particularly sweat, have variable and/or acidic pH, 3× PBS pH

https://doi.org/10.1021/jacs.2c02323
J. Am. Chem. Soc. 2022, 144, 8480−8486

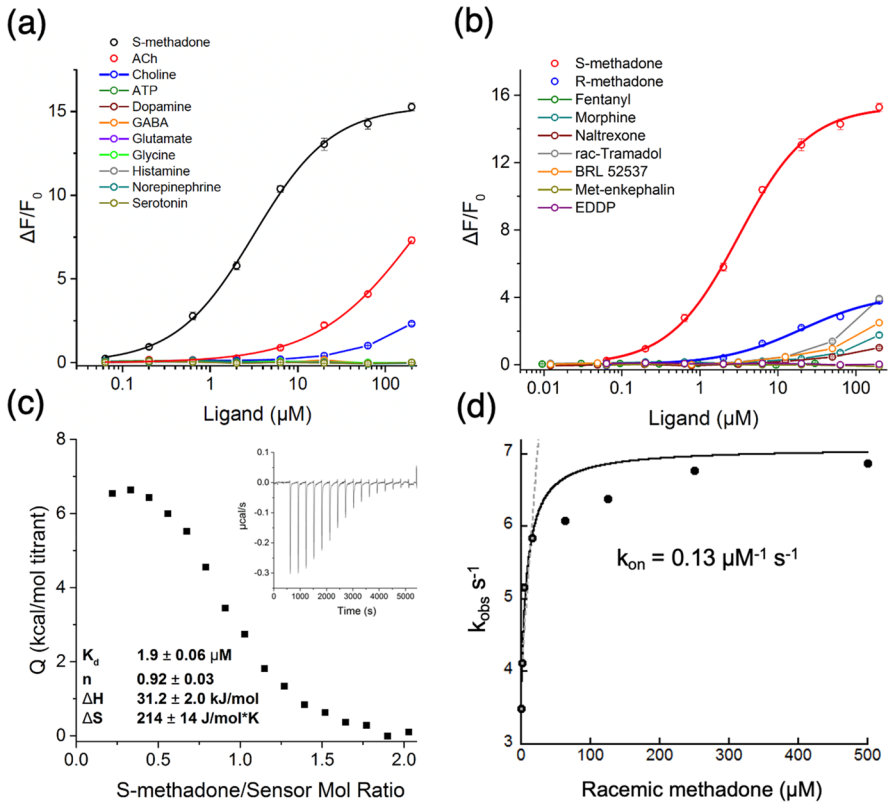

Figure 4. Selectivity and biophysical properties of iS-methadoneSnFR. (a) iS-methadoneSnFR vs endogenous neurotransmitters and choline. Responses to ACh and choline had S-slopes < 0.1 μM^{-1}. (b) iS-methadoneSnFR vs other clinically used opioids. The response to R-methadone was near zero at ~1 μM. Weak or no responses were observed for other drugs tested. EDDP is 2-ethylidene-1,5-dimethyl-3,3-diphenylpyrrolidine, the major metabolite of methadone. (c) Isothermal titration calorimetry of purified iS-methadoneSnFR. Thirty μM of the biosensor was mixed with 2 μL injections of 300 μM S-methadone. (d) Stopped-flow kinetic measurements with racemic methadone.

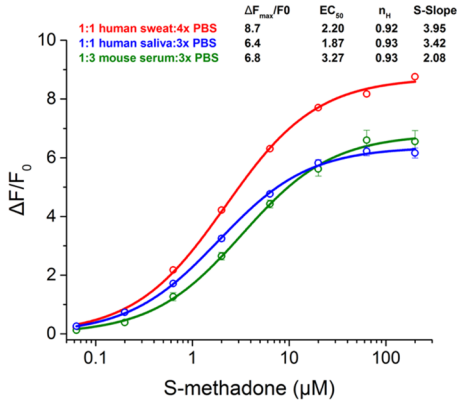

Figure 5. iS-methadoneSnFR dose−response relation in biofluids. 1:1 mixture of drug:biosensor in 3× PBS pH 7.4 with either human sweat or human saliva and 1:3 mixture with mouse serum (no pH adjustment of any biofluid).

7.4 was used to partially buffer a mixture with the biofluid. Still, the response at 1 μM and below in the biofluids provide at least ~200% dynamic range.

At the subcellular level, membrane-permeant weakly basic opioid drugs, but not impermeant derivatives or endogenous opioid peptides, enter the endoplasmic reticulum, and can act as pharmacological chaperones, altering the folding and trafficking of their receptors.[10] Opioid drugs also activate their receptors in endosomes and the Golgi apparatus.[11] We targeted iS-methadoneSnFR to the plasma membrane (Figure 6a), endoplasmic reticulum (Figure 6b), and Golgi apparatus (Figure 6c) of HeLa cells using targeting sequences. We

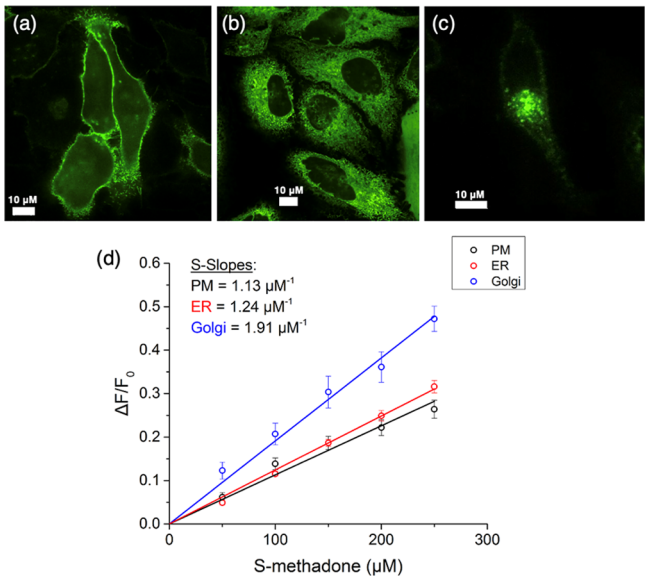

Figure 6. Spinning disk confocal imaging of HeLa cells transfected with (a) iS-methadoneSnFR_PM, (b) _ER, and (c) _Golgi (470 nm excitation, 535 nm emission, 100× 1.4 NA objective). Scale bar = 10 μm. (d) S-slope plotted for each organelle response at 0−250 nM S-methadone. Points are average responses to a 1 min pulse of [S-methadone]. PM n = 11 cells; ER n = 10; Golgi n = 11.

https://doi.org/10.1021/jacs.2c02323
J. Am. Chem. Soc. 2022, 144, 8480−8486

applied pulses of S-methadone (0 to 250 nM in 50 nM steps) to measure the linear portion of the dose−response relation (S-slope) in widefield imaging (Figure S8). The results indicate that ample S-methadone is available in the ER for potential chaperoning. The Golgi showed the largest S-slope among the three compartments (1.7× that of PM), despite having the lowest pH (Figure 6d). After correcting the S-slope for pH dependence, we find an accumulation factor of 2.9× to 4.4× across the Golgi pH range of 6.3 to 6.8[30] (Figure S8). Accumulation of opioids such as methadone in acidic compartments[31] may lead to intensified G-protein coupled signaling. We also validated iS-methadoneSnFR for time-resolved measurements in primary hippocampal neurons, encouraging mechanistic studies in tissues and in vivo (Figure S9).

Along with other sensors of opioid signaling,[11,32] this study establishes the first genetically encoded fluorescent protein biosensor for an opioid drug, enabling real-time quantification. Furthermore, the enantioselectivity encourages biosensor development to investigate "chiral switching" of other drugs where a single enantiomer substitutes a clinically used racemate.[33] One enantiomer may serve previously unstudied indications. For example, S-methadone is now under clinical investigation as a rapidly acting antidepressant via nonopioid mechanism(s).[34] The directed evolution results demonstrate that the nicotinic PBP may be converted to detect non-nicotinic small molecule amines by tuning residues around the aromatic first shell. Drug biosensors in vivo can monitor drug concentration near receptors during administration by the experimenter or the subject, a common manipulation for studying mechanisms of reward, analgesia, and drug abuse. To meet immediate needs for diagnostics, iS-methadoneSnFR can also provide in situ readouts in the laboratory or home.

■ ASSOCIATED CONTENT

Supporting Information

The Supporting Information is available free of charge at https://pubs.acs.org/doi/10.1021/jacs.2c02323.

Experimental details, reagents, supporting experimental figures, and amino acid and nucleotide sequences of iS-methadoneSnFR (PDF)

■ AUTHOR INFORMATION

Corresponding Author

Henry A. Lester − *Division of Biology and Biological Engineering, California Institute of Technology, Pasadena, California 91106, United States*; Email: lester@caltech.edu

Authors

Anand K. Muthusamy − *Division of Biology and Biological Engineering and Division of Chemistry and Chemical Engineering, California Institute of Technology, Pasadena, California 91106, United States*; orcid.org/0000-0003-1041-914X

Charlene H. Kim − *Division of Biology and Biological Engineering, California Institute of Technology, Pasadena, California 91106, United States*

Scott C. Virgil − *Division of Chemistry and Chemical Engineering, California Institute of Technology, Pasadena, California 91106, United States*

Hailey J. Knox − *Division of Chemistry and Chemical Engineering, California Institute of Technology, Pasadena, California 91106, United States*

Jonathan S. Marvin − *Howard Hughes Medical Institute, Janelia Research Campus, Ashburn, Virginia 20147, United States*; orcid.org/0000-0003-2294-4515

Aaron L. Nichols − *Division of Biology and Biological Engineering, California Institute of Technology, Pasadena, California 91106, United States*

Bruce N. Cohen − *Division of Biology and Biological Engineering, California Institute of Technology, Pasadena, California 91106, United States*

Dennis A. Dougherty − *Division of Chemistry and Chemical Engineering, California Institute of Technology, Pasadena, California 91106, United States*; orcid.org/0000-0003-1464-2461

Loren L. Looger − *Howard Hughes Medical Institute, University of California, San Diego, San Diego, California 92093, United States*

Complete contact information is available at: https://pubs.acs.org/10.1021/jacs.2c02323

Funding

This work was supported by the National Institute on Drug Abuse (NIDA) Grant DA043829, National Institute of General Medical Sciences (NIGMS) Grant GM-123582, and Janelia Research Campus, HHMI. H.A.L. was supported by DA043829 and GM-123582. A.K.M. was supported by DA043829, NIGMS fellowship 5T32GM007616, and National Institute of Neurological Disorders and Stroke fellowship T32NS105595. D.A.D. and H.J.K. were supported by the Tobacco-Related Disease Research Program (TRDRP) Grant T29IR0455. A.L.N. was supported by TRDRP fellowship 27FT-0022. L.L.L. and J.S.M. were supported by Janelia Research Campus, HHMI.

Notes

The authors declare the following competing financial interest(s): Anand K. Muthusamy, Henry A. Lester, Loren L. Looger, and Jonathan S. Marvin have filed a patent application that includes iS-methadoneSnFR.

Constructs reported in this manuscript will be deposited in Addgene. Sequences and dose response metrics will be made available in a GitHub repository.

■ ACKNOWLEDGMENTS

The Caltech Center for Catalysis and Chemical Synthesis supported by the Beckman Institute supported the chiral resolution work. Dr. Viviana Gradinaru and the CLOVER Center at Caltech provided plasmids and advice for AAV production. mApple-Golgi-7 was a gift from Dr. Michael Davidson (Addgene plasmid #54907). Andres Collazo and Giada Spigolon manage the Biological Imaging Facility supported by the Beckman Institute and advised on confocal imaging. The Proteome Exploration Laboratory was supported by NIH OD010788, NIH OD020013, the Betty and Gordon Moore Foundation through Grant GBMF775, and the Beckman Institute at Caltech. Dr. Wei Gao, Dr. You Yu, and Heather Lukas gathered human sweat. We thank Dr. Luke Lavis for contributive discussions. We thank Dr. Aiden Aceves and Dr. Stephen Mayo for advice on docking, Theodore Chin for assistance in cloning, and Purnima Deshpande for excellent lab management.

REFERENCES

(1) Althoff, K. N.; Leifheit, K. M.; Park, J. N.; Chandran, A.; Sherman, S. G. Opioid-Related Overdose Mortality in the Era of Fentanyl: Monitoring a Shifting Epidemic by Person, Place, and Time. *Drug and Alcohol Dependence* **2020**, *216*, 108321.

(2) Dole, V. P. A Medical Treatment for Diacetylmorphine (Heroin) Addiction. *J. Am. Med. Assoc.* **1965**, *193* (8), 646−650.

(3) Dole, V. P. Methadone Maintenance Treatment for 25,000 Heroin Addicts. *J. Am. Med. Assoc.* **1971**, *215* (7), 1131−1134.

(4) *Handbook of Methadone Prescribing and Buprenorphine Therapy*, 1st ed.; Cruciani, R., Knotkova, H., Eds.; Springer: New York, NY.

(5) Eap, C. B.; Buclin, T.; Baumann, P. Interindividual Variability of the Clinical Pharmacokinetics of Methadone: Implications for the Treatment of Opioid Dependence. *Clinical Pharmacokinetics* **2002**, *41* (14), 1153−1193.

(6) Li, Y.; Kantelip, J.-P.; Schieveen, P. G.; Davani, S. Interindividual Variability of Methadone Response: Impact of Genetic Polymorphism. *Mol. Diag Ther* **2008**, *12* (2), 109−124.

(7) Nilsson, M.-I.; Grönbladh, L.; Widerlöv, E.; Anggård, E. Pharmacokinetics of Methadone in Methadone Maintenance Treatment: Characterization of Therapeutic Failures. *Eur. J. Clin Pharmacol* **1983**, *25* (4), 497−501.

(8) Foster, D. J. R.; Somogyi, A. A.; Dyer, K. R.; White, J. M.; Bochner, F. Steady-State Pharmacokinetics of (R)- and (S)-Methadone in Methadone Maintenance Patients: Pharmacokinetics of (R)- and (S)-Methadone. *Br. J. Clin. Pharmacol.* **2000**, *50* (5), 427−440.

(9) Lester, H. A.; Miwa, J. M.; Srinivasan, R. Psychiatric Drugs Bind to Classical Targets Within Early Exocytotic Pathways: Therapeutic Effects. *Biol. Psychiatry* **2012**, *72* (11), 907−915.

(10) Petäjä-Repo, U. E.; Lackman, J. J. Targeting Opioid Receptors with Pharmacological Chaperones. *Pharmacol. Res.* **2014**, *83*, 52−62.

(11) Stoeber, M.; Jullié, D.; Lobingier, B. T.; Laeremans, T.; Steyaert, J.; Schiller, P. W.; Manglik, A.; von Zastrow, M. A Genetically Encoded Biosensor Reveals Location Bias of Opioid Drug Action. *Neuron* **2018**, *98* (5), 963−976.

(12) Ahmed, S. R.; Chand, R.; Kumar, S.; Mittal, N.; Srinivasan, S.; Rajabzadeh, A. R. Recent Biosensing Advances in the Rapid Detection of Illicit Drugs. *TrAC Trends in Analytical Chemistry* **2020**, *131*, 116006.

(13) Hudson, M.; Stuchinskaya, T.; Ramma, S.; Patel, J.; Sievers, C.; Goetz, S.; Hines, S.; Menzies, E.; Russell, D. A. Drug Screening Using the Sweat of a Fingerprint: Lateral Flow Detection of Δ9-Tetrahydrocannabinol, Cocaine, Opiates and Amphetamine. *Journal of Analytical Toxicology* **2019**, *43* (2), 88−95.

(14) Ardeshiri, M.; Jalali, F. Highly Selective Electrode for Potentiometric Analysis of Methadone in Biological Fluids and Pharmaceutical Formulations. *Materials Science and Engineering: C* **2016**, *63*, 30−36.

(15) Rezaei, B.; Tajaddodi, A.; Ensafi, A. A. An Innovative Highly Sensitive Electrochemical Sensor Based on Modified Electrode with Carbon Quantum Dots and Multiwall Carbon Nanotubes for Determination of Methadone Hydrochloride in Real Samples. *Anal. Methods* **2020**, *12* (43), 5210−5218.

(16) Khorablou, Z.; Shahdost-Fard, F.; Razmi, H. Flexible and Highly Sensitive Methadone Sensor Based on Gold Nanoparticles/Polythiophene Modified Carbon Cloth Platform. *Sens. Actuators, B* **2021**, *344*, 130284.

(17) Bick, M. J.; Greisen, P. J.; Morey, K. J.; Antunes, M. S.; La, D.; Sankaran, B.; Reymond, L.; Johnsson, K.; Medford, J. I.; Baker, D. Computational Design of Environmental Sensors for the Potent Opioid Fentanyl. *eLife* **2017**, *6*, No. e28909.

(18) Marvin, J. S.; Borghuis, B. G.; Tian, L.; Cichon, J.; Harnett, M. T.; Akerboom, J.; Gordus, A.; Renninger, S. L.; Chen, T.-W.; Bargmann, C. I.; Orger, M. B.; Schreiter, E. R.; Demb, J. B.; Gan, W.-B.; Hires, S. A.; Looger, L. L. An Optimized Fluorescent Probe for Visualizing Glutamate Neurotransmission. *Nat. Methods* **2013**, *10* (2), 162−170.

(19) Shivange, A. V.; Borden, P. M.; Muthusamy, A. K.; Nichols, A. L.; Bera, K.; Bao, H.; Bishara, I.; Jeon, J.; Mulcahy, M. J.; Cohen, B.; O'Riordan, S. L.; Kim, C.; Dougherty, D. A.; Chapman, E. R.; Marvin, J. S.; Looger, L. L.; Lester, H. A. Determining the Pharmacokinetics of Nicotinic Drugs in the Endoplasmic Reticulum Using Biosensors. *J. Gen. Physiol.* **2019**, *151* (6), 738−757.

(20) Borden, P. M.; Zhang, P.; Shivange, A. V.; Marvin, J. S.; Cichon, J.; Dan, C.; Podgorski, K.; Figueiredo, A.; Novak, O.; Tanimoto, M.; Shigetomi, E.; Lobas, M. A.; Kim, H.; Zhu, P. K.; Zhang, Y.; Zheng, W. S.; Fan, C.; Wang, G.; Xiang, B.; Gan, L.; Zhang, G.-X.; Guo, K.; Lin, L.; Cai, Y.; Yee, A. G.; Aggarwal, A.; Ford, C. P.; Rees, D. C.; Dietrich, D.; Khakh, B. S.; Dittman, J. S.; Gan, W.-B.; Koyama, M.; Jayaraman, V.; Cheer, J. F.; Lester, H. A.; Zhu, J. J.; Looger, L. L. A Fast Genetically Encoded Fluorescent Sensor for Faithful in Vivo Acetylcholine Detection in Mice, Fish, Worms and Flies. *bioRxiv*, February 8, 2020. DOI: 10.1101/2020.02.07.939504 (accessed on December 1, 2021).

(21) Tian, L.; Hires, S. A.; Mao, T.; Huber, D.; Chiappe, M. E.; Chalasani, S. H.; Petreanu, L.; Akerboom, J.; McKinney, S. A.; Schreiter, E. R.; Bargmann, C. I.; Jayaraman, V.; Svoboda, K.; Looger, L. L. Imaging Neural Activity in Worms, Flies and Mice with Improved GCaMP Calcium Indicators. *Nat. Methods* **2009**, *6* (12), 875−881.

(22) Larsen, A. A.; Tullar, B. F.; Elpern, B.; Buck, J. S. The Resolution of Methadone and Related Compounds. *J. Am. Chem. Soc.* **1948**, *70* (12), 4194−4197.

(23) Bera, K.; Kamajaya, A.; Shivange, A. V.; Muthusamy, A. K.; Nichols, A. L.; Borden, P. M.; Grant, S.; Jeon, J.; Lin, E.; Bishara, I.; Chin, T. M.; Cohen, B. N.; Kim, C. H.; Unger, E. K.; Tian, L.; Marvin, J. S.; Looger, L. L.; Lester, H. A. Biosensors Show the Pharmacokinetics of S-Ketamine in the Endoplasmic Reticulum. *Front. Cell. Neurosci.* **2019**, *13*, 499.

(24) Zeisel, S. H.; Epstein, M. F.; Wurtman, R. J. Elevated Choline Concentration in Neonatal Plasma. *Life Sciences* **1980**, *26* (21), 1827−1831.

(25) Faessel, H. M.; Obach, R. S.; Rollema, H.; Ravva, P.; Williams, K. E.; Burstein, A. H. A Review of the Clinical Pharmacokinetics and Pharmacodynamics of Varenicline for Smoking Cessation. *Clinical Pharmacokinetics* **2010**, *49* (12), 799−816.

(26) Russell, M. A.; Jarvis, M.; Iyer, R.; Feyerabend, C. Relation of Nicotine Yield of Cigarettes to Blood Nicotine Concentrations in Smokers. *BMJ.* **1980**, *280* (6219), 972−976.

(27) Nichols, A. L.; Blumenfeld, Z.; Fan, C.; Luebbert, L.; Blom, A. E. M.; Cohen, B. N.; Marvin, J. S.; Borden, P. M.; Kim, C. H.; Muthusamy, A. K.; Shivange, A. V.; Knox, H. J.; Campello, H. R.; Wang, J. H.; Dougherty, D. A.; Looger, L. L.; Gallagher, T.; Rees, D. C.; Lester, H. A. Fluorescence Activation Mechanism and Imaging of Drug Permeation with New Sensors for Smoking-Cessation Ligands. *eLife* **2022**, DOI: 10.7554/eLife.74648.

(28) Chung, M.; Fortunato, G.; Radacsi, N. Wearable Flexible Sweat Sensors for Healthcare Monitoring: A Review. *J. R. Soc. Interface.* **2019**, *16* (159), 20190217.

(29) Soares Nunes, L. A.; Mussavira, S.; Sukumaran Bindhu, O. Clinical and Diagnostic Utility of Saliva as a Non-Invasive Diagnostic Fluid: A Systematic Review. *Biochem Med.* **2015**, *25* (2), 177−192.

(30) Rivinoja, A.; Pujol, F. M.; Hassinen, A.; Kellokumpu, S. Golgi pH, Its Regulation and Roles in Human Disease. *Ann. Med.* **2012**, *44* (6), 542−554.

(31) De Duve, C.; De Barsy, T.; Poole, B.; Trouet, A.; Tulkens, P.; Van Hoof, F. Lysosomotropic Agents. *Biochem. Pharmacol.* **1974**, *23* (18), 2495−2531.

(32) Abraham, A. D.; Casello, S. M.; Schattauer, S. S.; Wong, B. A.; Mizuno, G. O.; Mahe, K.; Tian, L.; Land, B. B.; Chavkin, C. Release of Endogenous Dynorphin Opioids in the Prefrontal Cortex Disrupts Cognition. *Neuropsychopharmacol* **2021**, *46* (13), 2330−2339.

(33) Long, A. S.; Zhang, A. D.; Meyer, C. E.; Egilman, A. C.; Ross, J. S.; Wallach, J. D. Evaluation of Trials Comparing Single-Enantiomer Drugs to Their Racemic Precursors: A Systematic Review. *JAMA Netw Open* **2021**, *4* (5), No. e215731.

(34) Fogaça, M. V.; Fukumoto, K.; Franklin, T.; Liu, R.-J.; Duman, C. H.; Vitolo, O. V.; Duman, R. S. N-Methyl-D-Aspartate Receptor Antagonist d-Methadone Produces Rapid, MTORC1-Dependent Antidepressant Effects. *Neuropsychopharmacol* **2019**, *44* (13), 2230−2238.

https://doi.org/10.1021/jacs.2c02323
J. Am. Chem. Soc. 2022, 144, 8480−8486